Venhaus, Martin; Behn, Carsten; Freitag, Lutz; Zimmermann, Klaus:

Simulations and experiments of the balloon dilatation of airway stenoses

Zuerst erschienen in:	Biomedizinische Technik = Biomedical Engineering. - Berlin [u.a.] : de Gruyter. - 54 (2009), 4, p. 187-195.
Erstveröffentlichung:	2009-07-14
ISSN (online):	1862-278X
ISSN (print):	0013-5585
DOI:	10.1515/BMT.2009.022
[*Zuletzt gesehen:*	43696]

Biomed Tech 2009; 54:187–195 © 2009 by Walter de Gruyter • Berlin • New York. DOI 10.1515/BMT.2009.022

Simulations and experiments of the balloon dilatation of airway stenoses

Simulationen und Experimente zur Ballondilatation von Atemwegstenosen

Martin Venhaus[1,*], Carsten Behn[2], Lutz Freitag[3] and Klaus Zimmermann[2]

[1] Adept Technology GmbH, Dortmund, Germany
[2] Technische Universität Ilmenau, Fakultät für Maschinenbau, Fachgebiet Technische Mechanik, Ilmenau, Germany
[3] Oxygain Institute, Hemer, Germany

Abstract

This article investigates the mechanics of balloon dilatation in the treatment of bronchotracheal stenosis. The "scar stricture"-type stenosis examined in this paper is typically dilated manually, using a dilatation balloon. If indicated, this is followed by stent implantation. The selection of the stent with proper characteristics is performed empirically, based on personal experience and preference. In order to optimize the therapeutic outcome, however, it is necessary to match the stent with the stress-strain properties of the stenosis, which are not determined during manual balloon dilatation. The objective is to utilize models to experimentally and theoretically establish the correlation between the pressure/volume curve measured during the dilatation and the stress-strain properties of the stenosis, taking into account that during dilatation of scar strictures the balloon is only partially compressed, as it extends beyond both ends of the stenosis. Experiments are carried out using stenosis models with various extensibilities and lengths. As expected, more hardened stenosis resulted in steeper pressure/volume curves during the dilatation. On the other hand, the comparison between stenosis of equal extensibilities, but different length, showed an initially unexpected larger distension of the shorter stenosis, at equal pressure increases. This is caused by the fact that the margins of the stenosis are allowed more time to distend, compared to the central areas of the stenosis. The term "effect of margin expansion" was introduced to describe this behavior. The modeling of the dilatation process is based on the equilibrium conditions of cut-free balloon portions. The balloon/stenosis system is divided into three areas with different characteristics: (1) the proximal and distal area of the balloon outside the stenosis; (2) the area of contact between the balloon and the stenosis; and (3) the transition area between (1) and (2). Numerical simulations of the balloon dilatation confirm the conclusions from the experimental results and the theoretical considerations regarding the correlation between the pressure/volume curve of the dilatation and the stress-strain properties of the stenosis.

Keywords: balloon dilatation; experiments; simulation; stenosis; stent.

*Corresponding author: Dr. Martin Venhaus, Adept Technology GmbH, 44227 Dortmund, Germany
Phone: +49-(0)2334-520952
Fax: +49-(0)231-47739650
E-mail: m.venhaus@online.de

Zusammenfassung

Dieser Artikel befasst sich mit den mechanischen Vorgängen während der Ballondilatation von Atemwegstenosen. Die betrachteten Stenosen vom Typ „narbige Striktur" werden im klinischen Alltag üblicherweise mit dem Instrument Dilatationsballon manuell gedehnt. Falls notwendig, erfolgt eine anschließende Stentimplantation. Die Auswahl des Stents, inklusive seiner Kennlinie, erfolgt gefühlsmäßig oder nach persönlichen Erfahrungen und Präferenzen. Zur Erlangung eines optimalen Behandlungsresultates ist jedoch eine Anpassung an das Spannungs-Dehnungs-Verhalten der Stenose notwendig. Dieses Verhalten wird während der manuell durchgeführten Ballondilatation nicht ermittelt. Das Ziel dieser Studie ist, die Zusammenhänge zwischen dem während der Dilatation gemessenen Druck-Volumen-Verlauf und dem Spannungs-Dehnungs-Verhalten der Stenose experimentell und theoretisch auf Basis von Modellen zu bestimmen. Dabei wird die Besonderheit berücksichtigt, dass bei der Dehnung der narbigen Striktur der Dilatationsballon durch die Stenose nur teilweise eingeengt wird; er ragt an beiden Enden über den stenosierten Bereich hinaus. Es werden experimentelle Untersuchungen an Modellstenosen unterschiedlicher Dehnbarkeit und Länge durchgeführt. Wie erwartet, führen härtere Stenosen zu einem steileren Kurvenanstieg während der Dilatationsphase. Demgegenüber zeigt der Vergleich zwischen Stenosen gleicher Dehnbarkeit, aber unterschiedlicher Länge, eine zunächst unerwartet größere Dehnung der kürzeren Stenose bei gleicher Druckzunahme. Ursache ist, dass die Randbereiche der Stenosen einen zeitlichen Dehnungsvorsprung gegenüber den weiter innen liegenden Bereichen erfahren. Für dieses, bei kürzeren Stenosen ausgeprägtere Verhalten wird der Begriff „Effekt der Randdehnung" eingeführt. Die Modellbildung des Dilatationsvorganges basiert auf Gleichgewichtsbetrachtungen am freigeschnittenen Ballon. Das System Ballon/Stenose wird in drei Teilbereiche, für die unterschiedliche Bedingungen gelten, aufgeteilt. Die betrachteten Bereiche sind: 1. der proximale- und distale Ballonbereich außerhalb der Stenose; 2. der Bereich, in dem Ballon und Stenose in Kontakt treten; 3. der Übergangsbereich zwischen 1 und 2. Numerische Simulationen der Ballondilatation bestätigen die aus den experimentellen Untersuchungen und theoretischen Betrachtungen

gewonnenen Erkenntnisse über die Zusammenhänge zwischen Druck-Volumen-Verlauf der Dilatation und Spannungs-Dehnungs-Verhalten der Stenose.

Schlüsselwörter: Ballondilatation; Experimente; Simulation; Stenose; Stent.

Introduction

Stenoses of the airways have a considerable impact on the patient's quality of life due to a painful increased breathing load. Medical treatment is absolutely required. The type of treatment depends on the type of stenosis. These have been categorized by Freitag and Macha [6] as shown in a schematic diagram (Figure 1).

The scar stricture type stenosis is gaining in importance since they may result as an after-effect of intensive care medicine. Excessive granulation tissue induced by sharp edges of tracheal cannulas can be removed mechanically with a rigid bronchoscope. If there is not a life-threatening condition, it is usually removed by laser, argon-plasma coagulation or cryotherapy. The other type of sequella from long-term ventilation is submucosal scaring and shrinking of the tissue. In most cases, these are results from high circumferential cuff-pressures impairing mucosal perfusion. Only very short web scars can be cut with a laser. For the treatment of typical hourglass shaped strictures any cutting device is contraindicated. Careful dilatation, sometimes combined with stent placement, is the only reasonable alternative to surgical removal of a narrowed tracheal or bronchial segment. Therefore, only the scar stricture type stenosis is taken into account within this investigation.

Geometrically, this stenosis stretches across a well defined section and is constructed rotation-symmetrically with an approximately constant radius. To simplify, it can be described as a cylinder with the length L_{St} and the radius r_{St}. Typically, this type of stenosis is medicated by manual dilatation, using a dilatation balloon. If indicated, the treatment is followed by a stent implantation. During the dilatation the attending doctor observes the reset force of the syringe piston across the covered piston stroke (Figure 2).

Consciously or unconsciously the doctor believes in gaining information about the properties of the stenosis. However, this impression is adulterated by several influences:

- potential appearance of air blisters in the system syringe-catheter-balloon;
- expansion of the system syringe-catheter-balloon [13];
- flow rate depending pressure drop in the catheter [3];
- for biological materials the stress-strain relation is a function of time, and during manually operated dilatation the strain rate is more or less randomized [6, 7];
- the so far unconsidered mechanical effect that the margins of the stenosis are allowed more time to distend compared to the central areas of the stenosis; this will be described in the section "Modeling of the dilatation process".

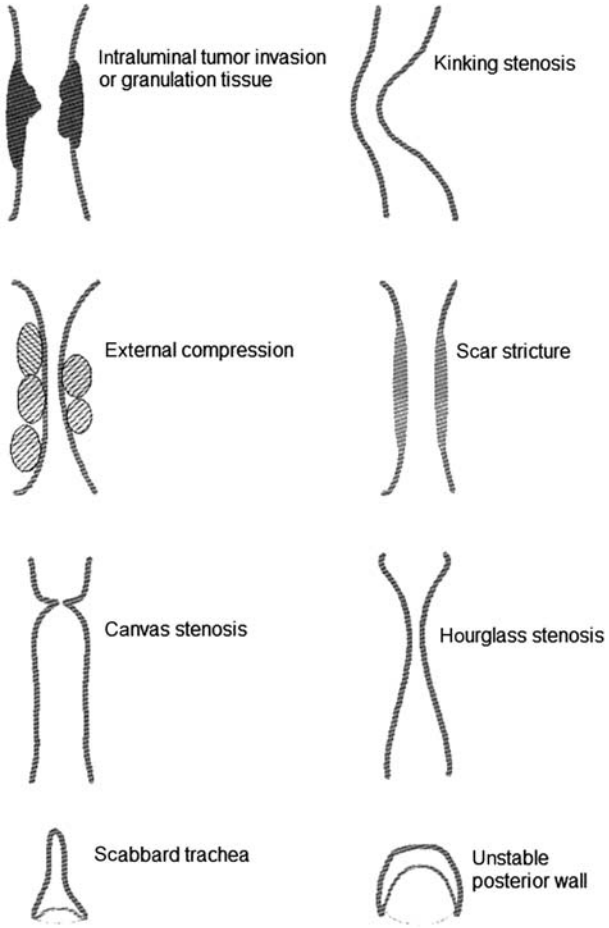

Figure 1 Categorization of the airway stenoses according to their appearance.
The type of treatment varies depending on the type of stenosis [6]. Only the scar stricture type stenosis is taken into account within this investigation.

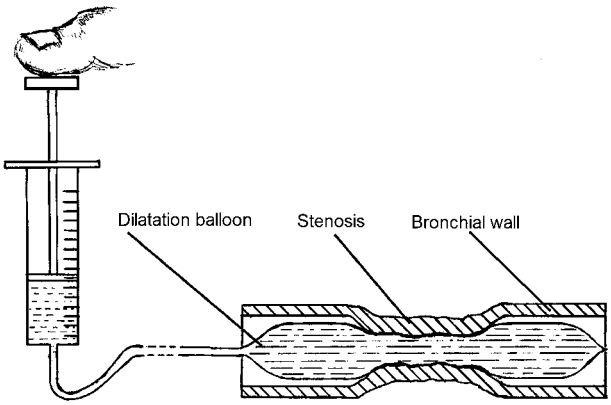

Figure 2 Schematic diagram of the manual balloon dilatation of a scar stricture type stenosis.
The reset force of the syringe across the covered piston stroke is felt in the thumb.

If the gain of distension has not turned out to be satisfactory, a subsequent stent implantation is indicated. In this regard, the biomechanics of the stenosis and the stent construction are coming into interaction. If a tracheal stent with an elastic characteristic is inserted into the stenosis, its reset force counteracts to the constric-

tion force of the stenosis. The obtained diameter results from the equilibrium conditions of those forces [6].

The mechanical characteristics of the stenosis differ significantly depending on the type of disease. The plurality of the available stents is confusing as well, the right choice is demanding. Apparently, this is done by personal preferences and commercial considerations, whereas mechanical aspects are considered secondarily [12].

It is obvious that additional knowledge about the stenosis characteristics is requested to assist the doctor in selecting the adequate stent. This request is emphasized by the increased quality awareness for healthcare [4, 10]. Ideally, the information gained during the dilatation would allow the calculation of the stress-strain property of the stenosis.

Materials and methods

Experimental set-up [11]

Experiments should clarify if a qualitative/quantitative relation between – during the dilatation of the stenosis measured – pressure/volume curves (*p*-*V*-curves) and the extensibilities of the stenosis exists.

In this regard, a standard plastic syringe (Typ B|Braun 5 ml) is connected to a computer-controlled linear axis which is normally used in industrial applications (manufacturer: Adept Technology Inc., Pleasonton, USA). This allows a programmable movement of the syringe piston and inflation of the dilatation balloon.

Pressure measurement during the balloon inflation was performed by a close to the syringe-outlet installed pressure sensor (manufacturer: fi-press, type: fi-press 610, Unterhaching, Germany). Therefore, the measured pressure is equivalent to the felt pressure during manual dilatation.

All experiments have been carried out using a low compliance balloon (LC-Balloon, "SMASH 10.0-40 5F", Boston Scientific, Natick, USA) with a diameter of 10 mm and a length of 40 mm. Figure 3 shows a snapshot during the dilatation of a stenosis model. Typical for the dilatation of scar strictures is that the balloon is only partially compressed, as it extends beyond both ends of the stenosis.

Plastic tubes with four different extensibilities and one metal tube have been used as model stenoses. All tubes had an inner diameter of 3.2 mm and a length of 10 mm and 20 mm, respectively. The *p*-*V*-curves for stenoses with a length of 10 mm are shown in Figure 4.

All curves can be broken down into the following three segments:

- Segment 1: the balloon is fully emptied, circumferential folded and under a slight low pressure (0 bar represents the air pressure in the laboratory). The linear axis is accelerated and the pressure reaches the 0 bar.
- Segment 2: the almost horizontal segment represents the filling phase where the balloon is not yet completely unfolded and the stenosis is not extended. At the end of the filling phase the two balloon parts outside the stenosis are unfolded and reach their cylindrical nominal form, whereas the mid-portion just touches the stenosis.
- Segment 3: the steeper part of the *p*-*V*-curves represents the actual dilatation process which extends the stenosis.
- The *p*-*V*-curves for stenoses with a length of 20 mm have a shorter filling phase; otherwise, they are comparable to the curves for the 10 mm stenoses.

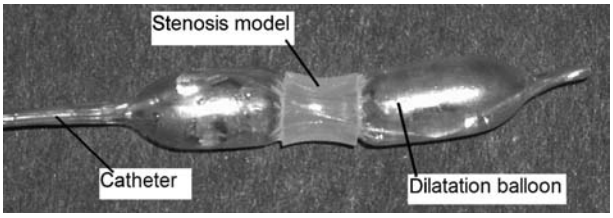

Figure 3 Snapshot during a dilatation of a stenosis model.

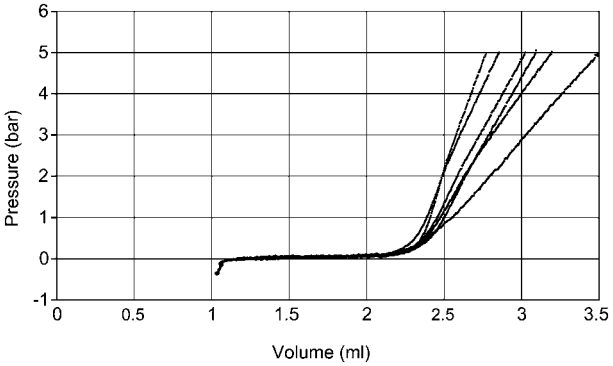

Figure 4 *p*-*V*-diagrams from dilatation of stenosis models with different extensibilities but identical lengths (10 mm).
The horizontal segments represent the filling phase, the steeper parts the dilatation process. More hardened stenosis results in steeper curves.

The pressure shown in the *p*-*V*-diagram is not identical to the pressure measured at the syringe-outlet. It shows the (calculated) pressure inside the balloon. In this regard, the pressure drop in the connection tube between syringe and balloon was subtracted from the measured pressure. The method described in [3] was used for verifying the presence of a laminar flow and to calculate the flow resistivity in the following way: assuming a laminar flow the Hagen-Poiseuille equation can be applied for the pressure drop Δp:

$$\Delta p = Q \frac{L}{A^2} \frac{8\pi}{\eta} \tag{1}$$

The flow rate Q, the length L of the connection tube and the viscosity η of the liquid (water) are known. There are no manufacturer's data about the cross-section surface A of the connection tube available and a measurement is not feasible.

Eq. (1) is further merged with R_s as the flow resistance:

$$R_s = \frac{L}{A^2} \frac{8\pi}{\eta} \tag{2}$$

$$\Delta p = Q \cdot R_s \tag{3}$$

Eq. (3) is also called "Ohm's law of hydrodynamics". Now the flow resistance *Rs* needs to be experimentally determined. Figure 5 shows test readings for the pressure drops Δp at six different flow rates *Q*. The measurements have been taken during the filling phase of the balloon, as during this phase the pressure at the end of connection tube is identical to the actual ambient pressure. The measured pressures therefore directly represent the pressure drop Δp.

According to "Ohm's law of hydrodynamics", the gradient of the line of best fit directly yields to the questioned flow resistance R_s:

$$R_s = 3.06 \frac{bar \cdot s}{ml}$$

The linear function confirms the expected laminar flow.

If possible, the increase of the volume shown in the *p-V*-diagram during the dilatation should be identical to the increase of the stenosis volume. The volume was determined by recording the piston movement and known piston diameter. However, this volume contains some additional objectionable volume increases caused by the extension of the syringe (plastic), the connection tube and the balloon hull. Potential air occlusion in the system can cause additional adulteration during the volume measurement. By plotting *p-V*-diagrams of the syringe at different piston position, it was possible to determine the unwanted additional volumes caused by the syringe and the air occlusion in the area of syringe/pressure-sensor. Effects based on the extension of the connection tube and the balloon hull have not been taken into consideration. Air conclusion in this area could be excluded after visual inspection.

The *p-V*-diagrams shown in Figures 4 and 6 are already corrected in pressure and volume by using the above described methods. They show a definite relation between the extensibility and curve characteristics: more hardened stenoses result in steeper pressure/volume curves during dilatation. This characteristic meets the expectations.

Figure 6 shows the *p-V*-diagrams of two stenosis models with different lengths ($l_1 = 10$ mm, $l_2 = 20$ mm) but otherwise identical characteristics (material, diameter). The filling phase for the shorter stenosis is longer because a bigger portion extends beyond both ends of the stenosis and need to be filled. The approximate parallelism of the two curves in the area of the dilatation process is unexpected for the following reason: since the balloon hull is not fully unfolded during the dilatation process, the internal balloon pressure p_{iBa} is directly transmitted through the balloon hull to the stenosis wall. The pressure to the stenosis wall is therefore identical to the internal balloon pressure.

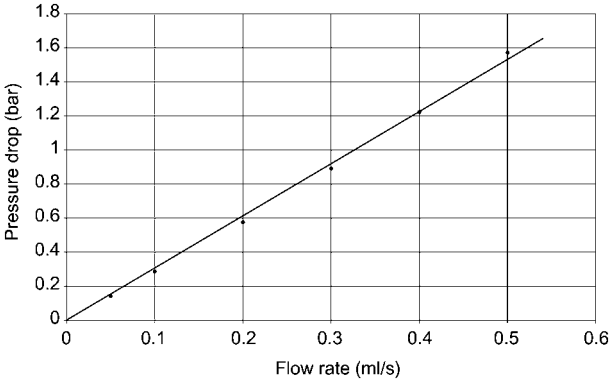

Figure 5 Function of "pressure drop-flow rate" in the connection tube.

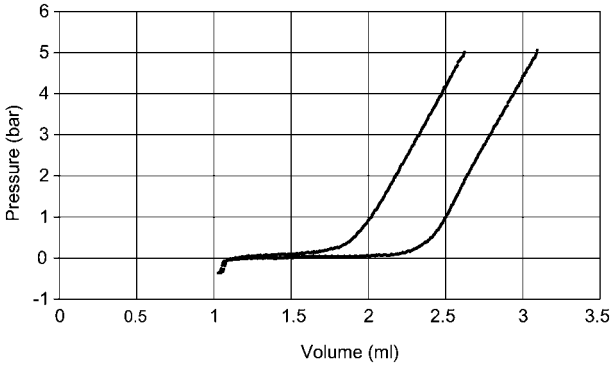

Figure 6 *p-V*-diagrams from dilatation of two stenosis models with different length but otherwise identical characteristics.
The shorter stenosis shows a longer filling phase. The approximate parallelism was initially unexpected.

Pressure increase Δp_i causes an increase of the stenosis diameter Δd_s through their entire length l_s. Under the assumption that the increase of the diameter Δd_s is identical over the length of the stenosis l_s, the longer stenosis should obtain a bigger increase of volume at equal pressure increase, with $\Delta V_1 < \Delta V_2$. In this case, the two *p-V*-curves in Figure 6 would not be parallel.

This is caused by the fact that the margins of the stenosis are allowed more time to distend, compared to the central areas of the stenosis. This behavior could be seen during the experiments (Figure 3) and on X-ray pictures during real dilatations of airway stenosis [6].

This will be analyzed in detail in the following section.

Modeling of the dilatation process [11]

Subsequent to the above experiments a mechanical model was developed and an assimilated set of equations was formed. Figure 7 shows a longitudinal cut of the balloon/stenosis system during the dilatation phase (snapshot). The sectional view of the balloon represents

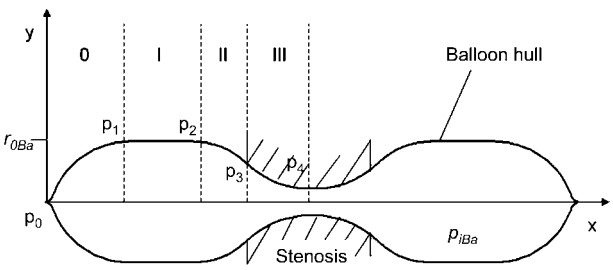

Figure 7 Longitudinal cut of the balloon/stenosis system during the dilatation phase (snapshot).
The function $y = f(x)$ built by the cross-section through the balloon hull is divided into four sections with different characteristics.

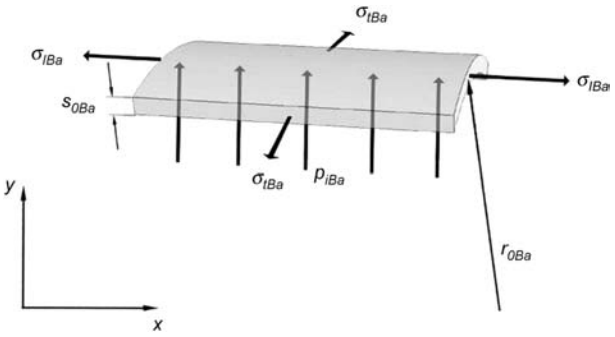

Figure 8 Equilibrium conditions for cut-free element from the balloon hull, section I.
In this section the balloon is completely unfolded.

a curve, where it is sufficient (properties of symmetry) to view the section between p_0 and p_4 only.

The function $y = f(x)$ can be divided into the sections 0, I, II, and III with different characteristics. To determine the mathematical inter-relationship, the modeling of the dilatation was based on the equilibrium conditions of cut-free balloon portions of the four different sections.

Section I This section is characterized by its cylindrical form (Figure 8). The known equations for closed cylindrical containers are applicable [9]. The stress is distributed uniformly across the hull thickness, since the hull thickness s_{0Ba} is small compared to the balloon diameter r_{0Ba}.

We therefore obtain for the axial stress:

$$\sigma_{lBa} = \frac{1}{2} p_{iBa} \frac{r_{0Ba}}{s_{0Ba}} \tag{4}$$

and for the circumferential stress:

$$\sigma_{tBa} = p_{iBa} \frac{r_{0Ba}}{s_{0Ba}} \tag{5}$$

Through the entire section I the function $y = f(x)$ is:

$$y = r_{0Ba} \tag{6}$$

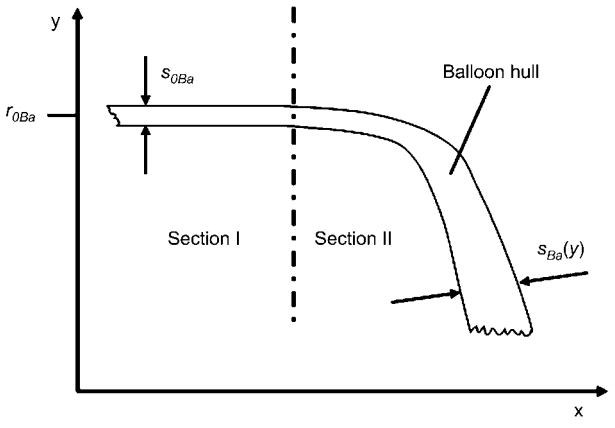

Figure 9 In section II (transition area) the balloon is not fully unfolded.
The balloon wall is built by several layers of the hull. This is reflected by a non-constant wall thickness $s_{Ba}(y)$.

Section II This section represents a "transition area". The balloon is not in contact with the stenosis. The balloon contraction in section III causes a non-cylindrical balloon shape in section II. Based on the longitudinal folding of the balloon hull, there is no circumferential tension in this section:

$$\sigma_{tBa} = 0 \tag{7}$$

The type of folding was not examined in detail. A uniform distribution of the material across the circumference was assumed instead (Figure 9). Under that assumption the balloon wall is built by (several) layers of the hull.

Geometric considerations lead to the following relation between the total wall thickness $s_{Ba}(y)$ and the y-coordinate:

$$s_{Ba}(y) = s_{0Ba} \frac{r_{0Ba}}{y} \tag{8}$$

Under the assumption that the axial stress is constant across the entire balloon hull, Eq. (4) can also be applied for section II:

$$\sigma_{lBa} = \frac{1}{2} p_{iBa} \frac{r_{0Ba}}{s_{0Ba}} \tag{9}$$

The application of the equilibrium conditions for the element shown in Figure 10 results in the following equitation for the axial stress:

$$\sigma_{lBa} = p_{iBa} \frac{r_{zBa}(y)}{s_{Ba}(y)} \tag{10}$$

Equalization of Eqs. (9) and (10) leads to:

$$p_{iBa} \frac{r_{zBa}(y)}{s_{Ba}(y)} = \frac{1}{2} p_{iBa} \frac{r_{0Ba}}{s_{0Ba}} \tag{11}$$

$$r_{zBa}(y) = \frac{1}{2} s_{Ba}(y) \frac{r_{0Ba}}{s_{0Ba}} \tag{12}$$

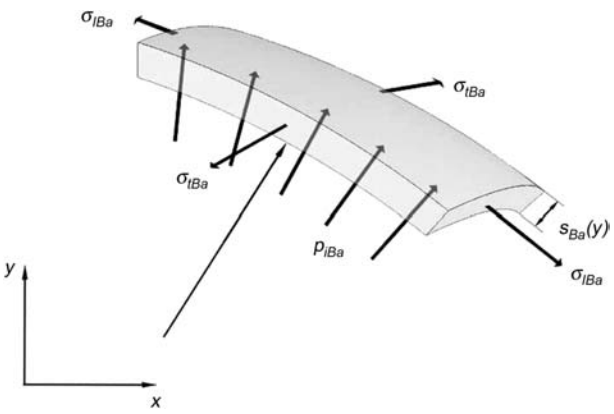

Figure 10 Equilibrium conditions for cut-free element from the balloon hull, section II (transition area).

Insertion from Eq. (8) for $s_{Ba}(y)$ results in:

$$r_{zBa}(y) = \frac{1}{2} s_{0Ba} \frac{r_{0Ba}}{y} \frac{r_{0Ba}}{s_{0Ba}} \tag{13}$$

After replacing the radius $r_{zBa}(y)$ by the reciprocal value of the curvature $k(y)$ under consideration of the sign (for section II, $k<0$) and some transformation we receive:

$$k_{zBa}(y) = -2y \frac{1}{r_{0Ba}^2} \tag{14}$$

The general equation for the curvature is:

$$k = \frac{y''}{(1+y'^2)^{3/2}} \tag{15}$$

Insertion of Eq. (15) into Eq. (14) results in a differential equation which characterizes section II:

$$\frac{y''}{(1+y'^2)^{3/2}} = -2y \frac{1}{r_{0Ba}^2} \tag{16}$$

For section II it turns out that the function $y=f(x)$ is independent of the internal balloon pressure p_{iBa} and the thickness of the balloon hull s_{0Ba} and $s_{Ba}(y)$, respectively.

Section III In this section the balloon and the stenosis are in direct contact with each other. Similar to section II there is no circumferential tension. The reason is again the longitudinal folding of the balloon hull, and therefore the same equations can be applied:

$$\sigma_{tBa} = 0 \tag{17}$$

$$s_{Ba}(y) = s_{0Ba} \frac{r_{0Ba}}{y} \tag{18}$$

Provided that the axial stress is constant across the entire balloon length, Eq. (4) is also valid for section III:

$$\sigma_{lBa} = \frac{1}{2} p_{iBa} \frac{r_{0Ba}}{s_{0Ba}} \tag{19}$$

The application of the equilibrium conditions for the element shown in Figure 11 results in the following equitation for the axial stress:

$$\sigma_{lBa} = (p_{St}(y) - p_{iBa}) \frac{r_{zBa}(y)}{s_{Ba}(y)} \tag{20}$$

In section III forces are transferred from the stenosis to the balloon and vice versa. A requirement for the application of the equilibrium conditions which are leading to 20 is that the forces are perpendicular to the surface of contact. Beyond doubt, this is valid for the forces caused by the internal balloon pressure. For the forces caused by the stenosis $p_{st}(y)$, absence of friction is required. Due to the wet mucosa, this can be taken for granted. For the experimental setup, the stenosis was rubbed in lube to gain absence of friction. Equating of Eqs. (19) and (20) results in:

$$(p_{St}(y) - p_{iBa}) \frac{r_{zBa}(y)}{s_{Ba}(y)} = \frac{1}{2} p_{iBa} \frac{r_{0Ba}}{s_{0Ba}} \tag{21}$$

After insertion of Eq. (8) for $s_{Ba}(y)$ we receive:

$$(p_{St}(y) - p_{iBa}) \frac{r_{zBa}(y) \cdot y}{s_{0Ba} \cdot r_{0Ba}} = \frac{p_{iBa} \cdot r_{0Ba}}{2 s_{0Ba}} \tag{22}$$

Transforming the equation results in:

$$p_{St}(y) - p_{iBa} = \frac{1}{r_{zBa}(y)} \frac{r_{0Ba}}{y} \frac{1}{2} p_{iBa} r_{0Ba} \tag{23}$$

Equivalent to section II the radius $r_{zBa}(y)$ is replaced by the reciprocal value of the curvature $k(y)$, whereas $k>0$ for this section.

$$p_{St}(y) - p_{iBa} = k_{zBa}(y) r_{0Ba}^2 \frac{1}{2y} p_{iBa} \tag{24}$$

Insertion of Eq. (15) into Eq. (24) and further transforming leads to a differential equation which characterizes section III:

$$p_{St}(y) - p_{iBa} - p_{iBa} \frac{1}{2y} r_{0Ba}^2 \frac{y''}{(1+y'^2)^{3/2}} = 0 \tag{25}$$

Section 0 In this section the balloon tapers off from its primarily cylindrical shape. Detailed information about the function $y=f(x)$ is not available. The shape forming is conditional of manufacturing. Considerations equivalent to those done for section II show that the function $y=f(x)$ is independent of the internal balloon pressure p_{iBa} and the thickness of the balloon hull s_{0Ba} and $s_{Ba}(y)$ as well. Therefore, it has a constant volume during the dilatation process. As a feasible simplification the peaked balloon shape is replaced by a cylindrical shape with a radius of r_{0Ba}. The length of the cylinder is chosen such that its volume is equal to the volume of the original body.

Summarizing we have to consider the following set of ordinary differential equations:

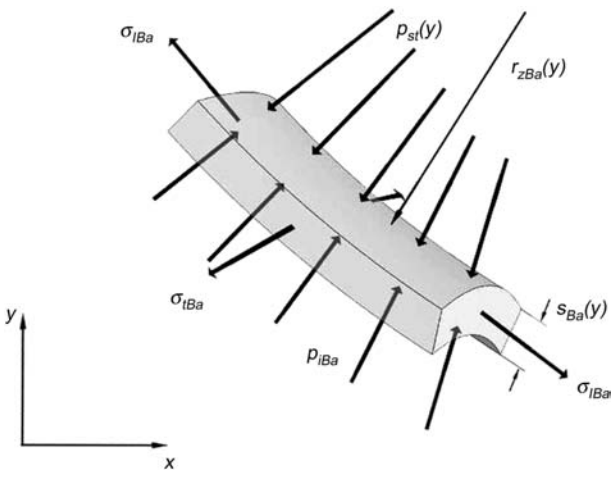

Figure 11 Equilibrium conditions for cut-free element from the balloon hull, section III.

$$y = r_{0Ba} \tag{26}$$

$$\frac{y''}{(1+y'^2)^{3/2}} = -2y\frac{1}{r_{0Ba}^2} \tag{27}$$

$$p_{St}(y) - p_{iBa} - p_{iBa}\frac{1}{2y}r_{0Ba}^2\frac{y''}{(1+y'^2)^{3/2}} = 0 \tag{28}$$

Boundary conditions: After finalizing the equations, respectively, the differential equations for the different sections of the function $y = f(x)$ and the additional boundary conditions need to be defined.

The nominal volume of the balloon is known by measurement and the nominal radius r_{0Ba} by the manufacturer's data. Due to the geometrical simplification done for section 0, the balloon can be considered as a continuous cylindrical body, as long as it is not compressed by the stenosis. The length L_{0Ba} of this cylindrical body can be calculated using the above data. The length L of the function $y = f(x)$ is constant during the entire dilatation process, provided that the balloon hull is inextensible. It is:

$$L = \int_{x_0}^{x_4} \sqrt{1 + [f'(x)]^2}\, dx \tag{29}$$

$$L = \frac{1}{2}L_{0Ba} \tag{30}$$

For sections 0, I, and II the lengths L_0, L_I, and L_{II} are unknown.

The length L_{III} for section III is identical with the length of the stenosis model. It is therefore constant and known.

The following information is known about the derivatives of the function $y = f(x)$:

Section 0: after converting this section to a cylindrical body, we receive $f'(x) = 0$ throughout this section.
Section I: we receive $f'(x) = 0$ across the entire section.
Section II: in point P_2 there is $f'(x_2) = 0$.
Section III: in point P_4 there is $f'(x_4) = 0$.

Observations lead to the assumption that point $P_3(x_3; y_3)$ is differentiable and continuous:

$$f'(x_3) = f'_r(x_3) = f'_l(x_3)$$

The equations and differential equations deducted in this section provide new knowledge about the mechanical process during the balloon dilatation of airway-stenoses. However, the examination of a snapshot during the dilatation process does not allow a direct calculation of the stress-strain properties of the stenoses based on the pressure/volume curve.

In the following section, it is attempted to further understand the correlation between the stress-strain properties of the stenosis and the pressure/volume curve from the dilatation by simulating the entire dilatation process.

Numerical simulations

Input data The set of ordinary differential equations and boundary conditions was transformed, following [8], and implemented in the software package "MATLAB" (Program package from the company "The MathWorks inc.", Version 6.5, Natick, USA).

Simulation parameters The chosen dimensions for the balloon and the stenoses have been identical to those of the experimental setup. Furthermore, eight different functions for describing the assumed stress-strain properties of the stenoses have been selected, namely linear and quadratic functions. Figure 12 shows the linear functions in graphical representation.

The elementary simulation results are described on the basis of an example. Dilated was a stenosis of the length $L_{St} = 10$ mm and the stress-strain properties described by the function $p_{StG3}(y)$ from Figure 12.

Figure 13 clearly shows the process of the balloon distention during the dilatation. The set of curves represents the function $y = f(x)$ for different pressures inside the balloon as described in the section "Modeling of the dilatation process". For symmetric reasons, only sections I, II, and III are displayed (see also Figure 7). Its curve progressing clearly shows that the margins of the stenosis are dilated first, whereas the central area of the stenosis is following time-delayed. The simulation confirms the "effect of margin expansion".

Rotation of the longitudinal cuts around the x-axis leads to the volume of the balloon at different pressures, and subsequently to the simulated pressure/volume curve (Figure 14). Unlike the measured pressure/volume curves ("Experimental set-up" section), the simulated curves only show the phase of dilatation. The filling phases remain unconsidered since they are not of relevance in this context.

Results

For a better understanding and evaluation of the simulation results, some of the pressure/volume curves have been combined in one diagram.

The comparison in Figure 15 shows that the stress-strain properties of the stenoses have a significant influ-

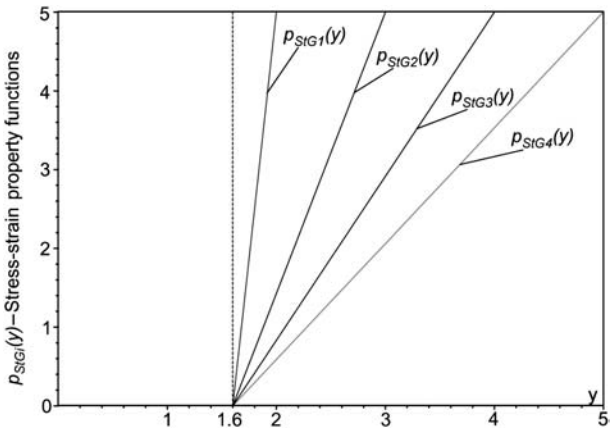

Figure 12 Different linear functions for the assumed stress-strain properties of the stenosis.
These functions have been used as input parameters for simulating the entire dilatation process. (Whereas "*St*" stands for "stenosis", and "*G*" for the German word "Gerade", which means "linear function".)

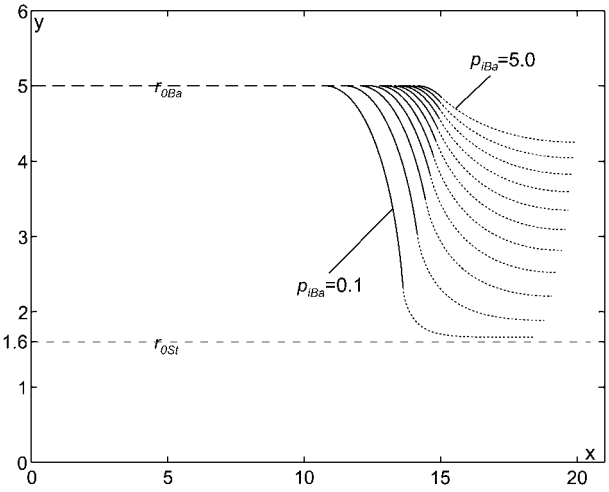

Figure 13 Longitudinal cuts of the balloon/stenosis system during a simulated dilatation at different pressures inside the balloon.
Only sections I (dashed), II (solid), and III (dotted) are displayed. Please compare to Figure 7.

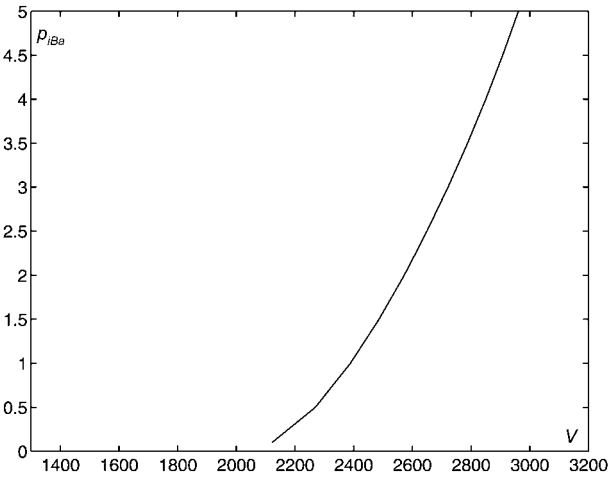

Figure 14 Pressure/volume curve calculated from the longitudinal cuts of the balloon/stenosis system (Figure 13).
Only the filling phase is displayed. Please compare to Figure 4.

ence to the run of the pressure/volume curves in the simulation as well. More hardened stenoses resulted in steeper pressure/volume curves. This behavior matches the pressure/volume curves from the experimental setup (Figure 4).

Compared to the experimental setup the stress-strain property of the stenoses is known for the simulation. This allows a further analysis of the pressure/volume curves from Figure 15. Assuming a linear stress-strain property, the pressure/volume curves from an idealized dilatation results in a quadratic function. An idealized dilatation means that the entire displaced volume (from moving the syringe piston) exclusively conducts to the dilatation of the stenosis. An idealized pressure/volume curve was exemplarily calculated for the dilatation of a stenosis with the length L_{st}=10 mm and the stress-strain property $P_{StG3}(y)$ from Figure 12.

The comparison between the idealized (Figure 16) and the simulated pressure/volume curves (Figure 15) show a significant difference in their characteristics, in spite of identical stress-strain properties of the stenoses:

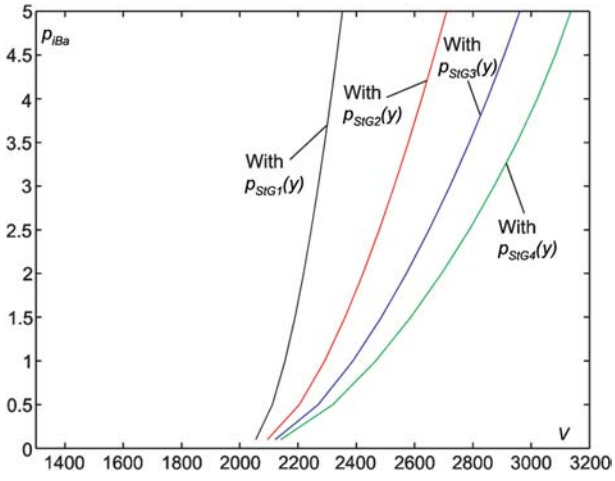

Figure 15 Pressure/volume curves belonging to the simulated dilatation for the four linear functions (stress-strain properties of the stenoses).
Only the filling phase is displayed. Length of the stenosis: 10 mm.

- The pressure/volume curve for the idealized dilatation represents a quadratic function with a negative curvature.
- For the simulated dilatation, the pressure/volume curve represents a function with a positive curvature.

This difference (exemplarily shown for a linear stress-strain property of the stenosis) is based on the fact that during dilatation of scar strictures the balloon is only partially compressed, as it extends beyond both ends of the stenosis.

Discussion, conclusion, and outlook

Three consecutive methods were applied to gain new knowledge about the correlation between the pressure/volume curve measured during the dilatation of the scar stricture and the stress-strain properties of the stenosis, taking into account that during dilatation of scar strictures the balloon is only partially compressed:

- experimental investigation;
- modeling;
- simulation.

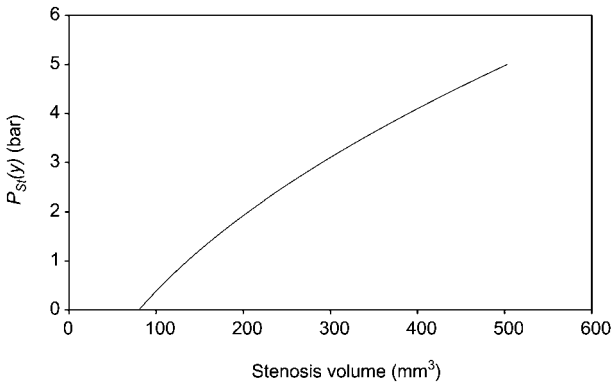

Figure 16 Pressure/volume curve for an idealized dilatation (the entire displaced volume exclusively conducts to the dilatation of the stenosis) of a stenosis with the length L_{st}=10 mm.

The experiments clearly demonstrated the influence of the stenosis extensibility to the *p*-*V*-diagrams curve progression. More hardened stenoses resulted in steeper pressure/volume curves during the dilatation.

The comparison of *p*-*V*-diagrams from stenoses with different length but otherwise identical characteristics showed a larger distension for the shorter stenosis, at equal pressure increases. This is caused by the "effect of margin expansion", which only appears if the length of the balloon exceeds the length of the stenosis, as is the case when dilating the scar stricture type stenosis. At all previously research works [2, 5] the balloon is fully surrounded by the stenosis, hence the "effect of margin expansion" did not appear.

The subsequently modeling observed a snapshot of the dilatation process only. Based on the equilibrium conditions of cut-free balloon portions, a set of ordinary differential equations and boundary conditions were developed. They lead to a full comprehension of the dilatation process with reference to the mechanical aspects. However, a snapshot only does not allow a complete calculation of the stenosis stress-strain properties. Using the knowledge gained from the experiments and modeling, the entire dilatation process was simulated. The simulation results are in good conformity with the experimental results. They clearly confirm the discovered "effect of margin expansion" which significantly influences the dilatation process and the run of the pressure/volume curve. With that a high risk of misinterpreting the feeling during manual dilatation is given.

However, the applied methods do not allow a straight calculation of the stenosis stress-strain properties. For this an additional mathematical approach (optimization process) needs to be developed.

During the clinical routine further consequences should be observed.

The "effect of margin expansion" can be avoided by using a dilatation balloon with the exact same length as the stenosis, and consequently the balloon needs to be placed very precisely in longitudinal direction which could lead to additional challenges.

The pressure/volume curve only represents the integral average. This does not allow determination of the viscoelastic behavior of the stenosis. All stenosis models examined by the authors have been of a cylindrical shape which is adequate for the scar stricture type stenosis, but other types of stenoses will lead to additional adulteration of the pressure/volume curve.

A general direction for further research should be the use of additional information from medical imaging during the dilatation process in combination with the findings from Abeszer and Steigenberger [1].

Acknowledgements

The authors are indebted to Joachim Steigenberger (Technische Universität Ilmenau) for fruitful and critical discussions.

References

[1] Abeszer H, Steigenberger J. Quasistatic inflation processes within rigid tubes. Preprint/Technische Universität Ilmenau, Institut für Mathematik; 06–09. Z Angew Math Mech 2008; 88: 556–572.

[2] Albrecht J. Biomechanische Modellierung und Konstruktion eines medizinisch-technischen Kontrollgerätes zur Qualitätsverbesserung der Koronar-Dilatation. Dissertation an der Universität Hannover. Hannover, Germany 1992.

[3] Bloß P, Werner C. Ein einfaches Modell zur Beschreibung von Druck-Volumen-Kurven bei freier Ballondilatation unter Berücksichtigung der Dynamik der Inflationshydraulik. Biomed Tech 2000; 45: 154–162.

[4] Bundesärztekammer. Curriculum Qualitätssicherung/Ärztliches Qualitätsmanagement. Köln: Arbeitsgemeinschaft der Deutschen Ärztekammern 2003.

[5] Demer L, Büchi A, Nishikawa R, Smalling RW, Gould KL. The use of pressure-volume curves to assess the mechanism and adequacy of stenosis dilatation by balloon angioplasty. Z Kardiol 1987; 76 (Suppl 6): 37–41.

[6] Freitag L, Macha HN. Biomechanik von Stenosen und Stents. In: Waßermann K. Interventionelle und diagnostische Bronchologie. München-Deisenhofen: Dustri-Verlag Dr. Karl Feistle 2000: 24–49.

[7] Fung YC. Biomechanics: mechanical properties of living tissues. 2nd edition. New York: Springer Verlag 1993.

[8] Hoffmann A, Marx B, Vogt W. Mathematik für Ingenieure 2. 1. Aufl. München: Pearson Studium 2006.

[9] Holzmann G, Dreyer HJ, Faiss H. Geschlossene dünnwandige zylindrische und kugelförmige Behälter unter innerem und äußerem Überdruck. In: Holzmann G, Meyer H, Schumpich G. Technische Mechanik. Teil 3 Festigkeitslehre. Stuttgart: B.G. Teubner 1979: 203–204.

[10] Silber S. Qualitätssicherung in der Kardiologie: Deutschland. Herz 1996; 21: 273–282.

[11] Venhaus M. Ein Beitrag zur Modellbildung und Simulation der Ballondilatation von Atemwegstenosen. Göttingen: Cuvillier 2007.

[12] Waßermann K. Stents – und ein skeptisches Plädoyer für die Palliativmedizin. In: Waßermann K. Interventionelle und diagnostische Bronchologie. München-Deisenhofen: Dustri-Verlag Dr. Karl Feistle 2000: 60–75.

[13] Werner C, Bloß P, Kießling D, Patschke H, Unverdorben M, Vallbracht C. Druck-Volumen-Messungen an PTCA-Kathetern mit Ballons niederer und höherer Compliance. Biomed Tech 1999; 44: 300–307.

Received June 18, 2008; accepted May 12, 2009; online first July 14, 2009